













DFT study on the interaction between carbon dioxide and doped fullerene C₃₀

Estudio computacional de la interacción entre dióxido de carbono y fullereno C₃₀ dopado

Toxqui-De La Torre, Ana Paulina^{*a}, Mandujano-Ramirez, Humberto Julián^b, Martinez-Vargas, Sergio^c and Patiño-Carachure, Cristóbal^d

- ^a  Universidad Autónoma del Carmen •  0009-0002-1103-2406 •  1322390
- ^b  Universidad Autónoma del Carmen •  0000-0003-3714-5564 •  266189
- ^c  Universidad Autónoma del Carmen •  0000-0002-2499-3970 •  100782
- ^d  Universidad Autónoma del Carmen •  0000-0002-1436-1259 •  226327

CONAHCYT classification: DOI: <https://doi.org/10.35429/H.2024.14.9.18>

Area: Engineering
Field: Engineering
Discipline: Materials Science and Technology
Subdiscipline: Materials Properties

Key Handbooks

The main contribution of this research involves the computational study of the nanostructure of Boron and Nitrogen doped C30 fullerene. Evaluating its adsorption energy, using density functional theory (DFT), by means of the PBE functional and the 6-31G(d,p) basis set. This study also obtains the HOMO and LUMO of each optimised doped nanostructure, as these can be used to determine the applications of a nanomaterial in both optical and electronic devices. The different doping sites influence the nanostructure of the fullerene, and see how it reacts with two family groups of different elements, and its adsorption energy in each of its doped and optimised nanostructures and how its geometric shape changes once it has been calculated. The adsorption energy of C30 and C29X (X=B, N) in the presence of CO² indicates that the doping site with some element is relevant in the optimisation process.

Citation: Toxqui-De La Torre, Ana Paulina, Mandujano-Ramirez, Humberto Julián, Martinez-Vargas, Sergio and Patiño-Carachure, Cristóbal. 2024. DFT study on the interaction between carbon dioxide and doped fullerene C₃₀. 9-18. ECORFAN.

* ✉ (153508@mail.unacar.mx)

Handbook shelf URL: <https://www.ecorfan.org/handbooks.php>

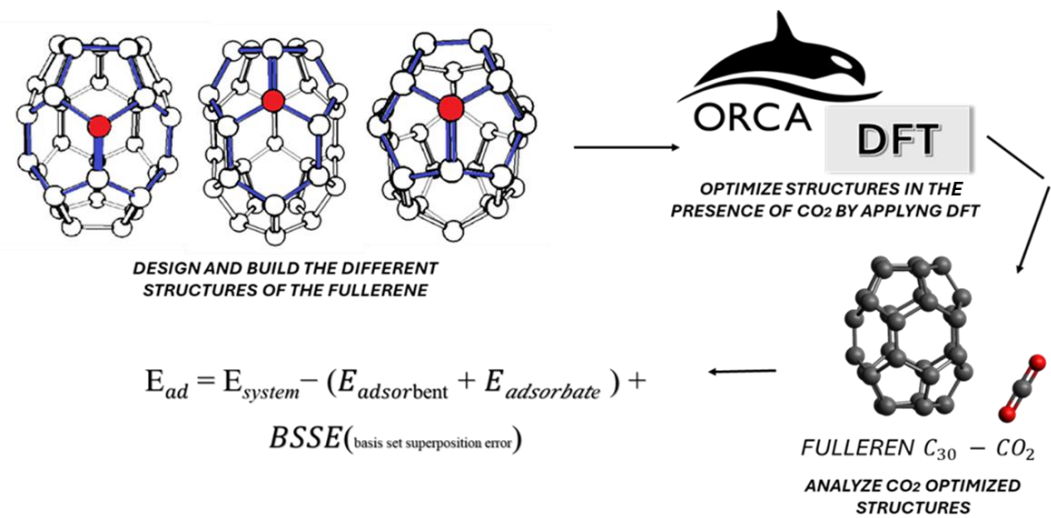


ISBN 978-607-8948-50-5/©2009 The Authors. Published by ECORFAN-Mexico, S.C. for its Holding Mexico on behalf of Handbook HRPG. This is an open access chapter under the CC BY-NC-ND license [<http://creativecommons.org/licenses/by-nc-nd/4.0/>]
Peer Review under the responsibility of the Scientific Committee MARVID®- in contribution to the scientific, technological and innovation Peer Review Process by training Human Resources for the continuity in the Critical Analysis of International Research.



Abstract

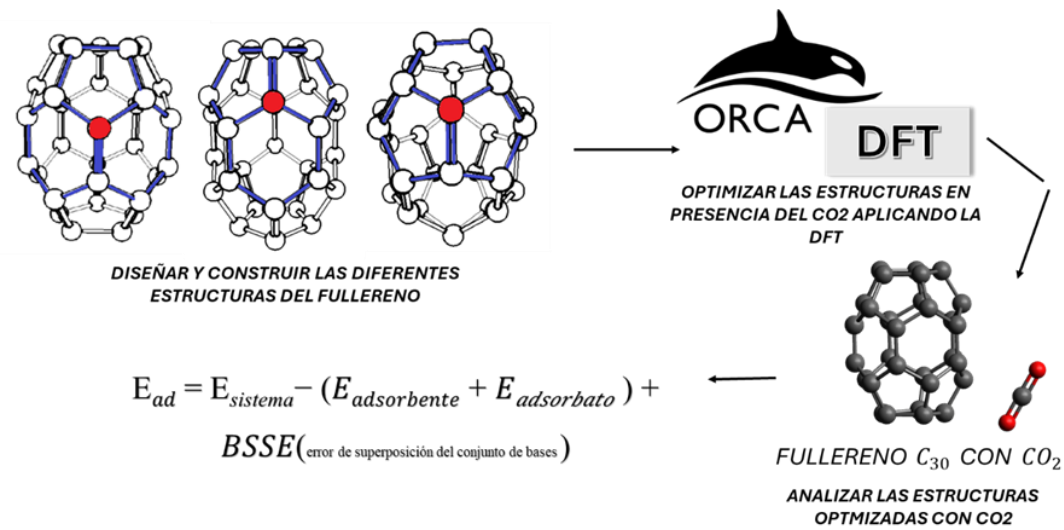
Fullerenes are symmetrical carbon nanostructures zero dimensional with hybridation sp²-bondend carbon atoms (with four valence electrons) arranged in pentagonal and hexagonal rings that form a hollow closed-cage structure. Fullerene C₃₀ is not symmetrical, specifically has 12 pentagonal and 5 hexagonal rings that form a barrel-like shape where the 5 hexagons form the body of the barrel, and the 12 pentagons are located in the bases of the barrel. Doped fullerenes were built by placing a heteroatom (as a boron or a nitrogen atom, with three or five valence electrons, respectively) at different doping sites. Doped fullerenes were optimized in presence of CO₂ using density functional theory (DFT) through PBE functional and 6-31G(d,p) basis set. The CO₂ adsorption energy on doped fullerenes were determined.



Fullerene doped, Carbon nanostructure, Absorption energy

Resumen

Los fullerenos son nanoestructuras de carbono simétricas de dimensión cero con átomos de carbono de enlace sp² de hibridación (con cuatro electrones de valencia) dispuestos en anillos pentagonales y hexagonales que forman una estructura hueca de jaula cerrada. El fullereno C₃₀ no es específicamente simétrico tiene 12 anillos pentagonales y 5 hexagonales que forman una forma parecida a un barril donde los 5 hexágonos son el cuerpo del barril y los 12 pentágonos están situados en las bases del barril. Los fullerenos dopados se construyeron colocando un heteroátomo (como un átomo de boro o de nitrógeno, con tres o cinco electrones de valencia, respectivamente) en diferentes sitios de dopaje. Los fullerenos dopados se optimizaron en presencia de CO₂ utilizando la teoría funcional de la densidad (DFT) mediante el funcional PBE y el conjunto de bases 6-31G(d,p). Se determinó la energía de adsorción de CO₂ en los fullerenos dopados.



Fullereno dopado, Nanoestructura de carbono, Energía de adsorción

Introduction

One of the materials that is of considerable interest at present is buckminsterfuller or better known as fullerene. C_{60} (fullerene) is a mainstay of research due to its physicochemical properties, making it the most studied fullerene. These characteristics make it particularly suitable for exploration in the fields of materials science and engineering.

In fullerenes there are σ bonds, formed by overlapping, where the electron density is concentrated between the nuclei of the atoms, and π bonds, resulting from the lateral overlapping of the orbitals, with the electron density distributed above and below the plane of the nuclei linked at the front of the orbitals. For this reason, fullerenes have a spherical shape called Bucky sphere (Tománek David, 2014). There is a greater diversity of fullerene structures, but not all of them have a spherical structure, such as C_{30} , which is smaller in size (Tománek David, 2014). (ver fig. 1).

Box 1

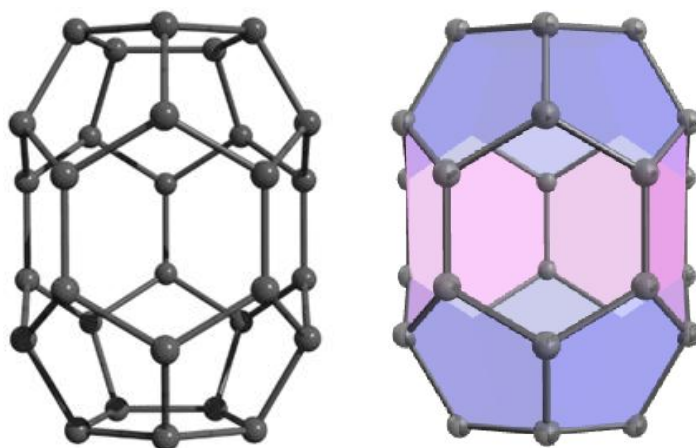


Figure 1

Modelling of the structure of C_{30} fullerene which is made up of 12 pentagons and 5 hexagons

Source: Own elaboration

Smaller fullerenes currently have more impact in the scientific literature due to their high potential in the development of advanced applications in key areas of nanotechnology and theoretical chemistry, and are an area of interest for the study of their properties and possible applications.

On the other hand, CO_2 adsorption on fullerenes is a very important area of study at present. Previously, adsorption of toxic gases has been studied with carbon nanostructures; nanotubes, graphene etc.

Most of the work reported in the scientific literature on doped fullerenes uses *Density Functional Theory* (DFT). DFT is a theory widely used to study molecular systems, nanostructures, solids and surfaces by solving approximate versions of the Schrödinger equation. Its origin dates back to an article by Hohenberg and Kohn in 1964 in *Physical Review*, entitled ‘Inhomogeneous Electron Gas’. Its methodology is used in a variety of fields and problems, with the study of electronic structure in the ground state being one of the most common. In this work, CO_2 adsorption on C_{30} and $C_{29}X$ ($X = B, N$) fullerenes at different doping sites was studied to obtain its adsorption energy (E_{Ad}), including the basis set error correction (BSSE).

Methodology

Design and construction of the different molecular structures

The fullerene structures were designed by constructing a barrel composed of carbon atoms, with single and double bonds. Unlike a common fullerene which has a spherical shape, C_{30} is composed of 12 pentagons and 5 hexagons.

The design has been made by forming the C_{30} fullerene structures, then replacing a carbon atom at different doping sites (see fig. 2) with Boron and Nitrogen to form the $C_{29}B$ and $C_{29}N$ structure. The CO_2 molecule was also constructed and each of them was optimised with the PBE functional, with the 6-31G(d,p) basis set.

Box 2

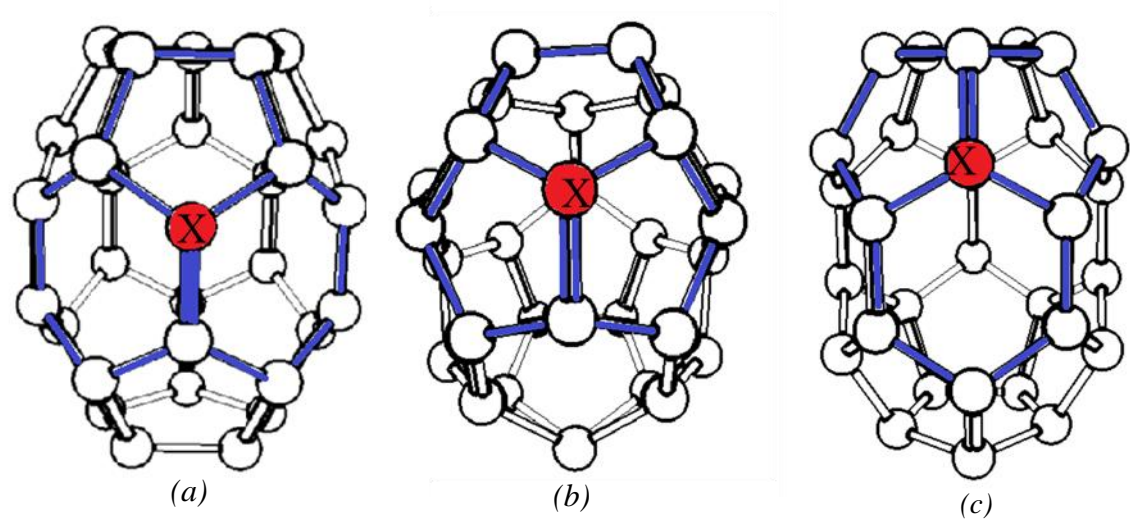


Figure 2
Doping sites. Element X is: (a) surrounded by 2 hexagonal rings and a pentagonal ring (PHH), (b) surrounded by three pentagonal rings (PPP) and (c) surrounded by 2 pentagonal rings and a hexagonal ring (PPH)
Source: Own elaboration

Optimisation of the structures in the presence of CO_2 by applying DFT.

The calculations were performed using ORCA 4.2.1 (Neese, F. 2022), as a first step the optimisation of the designed structures of C_{30} and $C_{29}X$ ($X= B, N$) was performed to determine the minimum energy of the most stable geometries, then the minimum energy of the interaction of the fullerenes with CO_2 was calculated, finally the adsorption energy was calculated. Figure 3 shows the optimised structure and the optimised structure with CO_2 .

Box 3

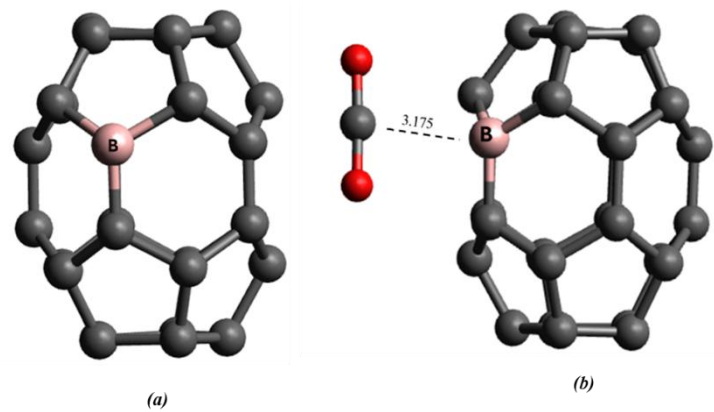


Figure 3
Optimised structure of boron-doped C_{30} fullerene (a)
Optimised structure of CO_2 -doped $C_{29}B$ (b)
Source: Own elaboration

The adsorption energies are calculated with the following equation. (Kahn, Ahmad, et al., 2021)

$$E_{Ad} = E_{sistema} - (E_{adsorbente} + E_{adsorbato}) + BSSE$$
 [1]

Where ($E_{sistema}$) is the system energy of the system corresponding to the minimum energy of the interaction of the C_{30} ó $C_{29}X$ ($X=B, N$) With the CO_2 , ($E_{adsorbente}$) is the adsorbent energy which corresponds to the basal state energy of the adsorbent. C_{30} y $C_{29}X$ ($X= B, N$), ($E_{adsorbato}$) is the minimum energy of the molecule of the CO_2 .

The term BSSE is the basis set superposition error, this calculation arises from molecular interactions. The calculation of the BSSE is of utmost importance because during the molecular interaction there are variations in the energy of each molecule due to the superposition of the wave functions of each molecule (Boys & Bernardi, 1970). We used the BSSE calculation methodology implemented in the ORCA software to calculate the interaction energy of C_{30} , $C_{29}X$ ($X=B, N$) and CO_2 which is obtained by the following equation:

$$BSSE = [E_{C_{30}}^{C_{30}-CO_2}(C_{30}) + E_{CO_2}^{C_{30}-CO_2}(CO_2)] - [E_{C_{30}}^{C_{30}-CO_2}(C_{30} - CO_2) + E_{CO_2}^{C_{30}-CO_2}(C_{30}-CO_2)] \quad [2]$$

Where, $E_{C_{30}}^{C_{30}-CO_2}(C_{30})$ is the energy of the C_{30} , obtained from the geometrical optimisation of the system $C_{30}-CO_2$ calculated on the basis of C_{30} , $E_{CO_2}^{C_{30}-CO_2}(CO_2)$ is the energy of the CO_2 , obtained from the geometrical optimisation of the system $C_{30}-CO_2$, calculated on the basis of CO_2 , $E_{C_{30}}^{C_{30}-CO_2}(C_{30} - CO_2)$ is the energy of the CO_2 obtained from the geometrical optimisation of the system $C_{30}-CO_2$ y $E_{CO_2}^{C_{30}-CO_2}(C_{30}-CO_2)$ is the energy of the CO_2 calculated from the optimisation of the system $C_{30}-CO_2$ obtained from the base of $C_{30}-CO_2$. Similarly, the basis set superposition error (BSSE) is computed for $C_{29}B-CO_2$ and $C_{29}N-CO_2$

Finally, the band gap energy is calculated from the energy of the highest occupied molecular orbital (*HOMO*) and the energy of the lowest unoccupied molecular orbital (*LUMO*).

Results

Minimum energies of C_{30} , $C_{29}X$ ($X=B, N$) interacting with CO_2

Table | shows the minimum energies of each of the C_{30} , $C_{29}X$ ($X=B, N$) structures interacting with CO_2 at different doping sites. Observing that the minimum energies at the different doping sites vary for each structure.

Box 4

Table 1
Doping sites and minimum energy of each of the systems C_{30} y $C_{29}X$ ($X=B, N$)

DOPING SITES	C ₂₉ X-CO ₂	SYSTEM ENERGY (eV)
PHH	C ₃₀ -CO ₂	-1329.69006
	C ₂₉ B-CO ₂	-1316.562063
	C ₂₉ N-CO ₂	-1346.407651
PPH	C ₃₀ -CO ₂	-1329.690815
	C ₂₉ B-CO ₂	-1316.584383
	C ₂₉ N-CO ₂	-1346.427076
PPP	C ₃₀ -CO ₂	-1329.689821
	C ₂₉ B-CO ₂	-1316.584383
	C ₂₉ N-CO ₂	-1346.432648

Source: Own elaboration

System $C_{30}-CO_2$

The energy of the $C_{30}-CO_0-CO_2$ system was calculated after optimisation. Figure 4 shows its adsorption energy at the doping sites from lowest to highest; two pentagonal rings and one hexagonal ring (*PPH*), two hexagonal rings and one pentagonal ring (*PHH*), three pentagonal rings (*PPP*). Observing that as the adsorption energy becomes more negative, the distance to the CO_2 molecule becomes shorter. This behaviour has an impact on the doping site.

Box 5

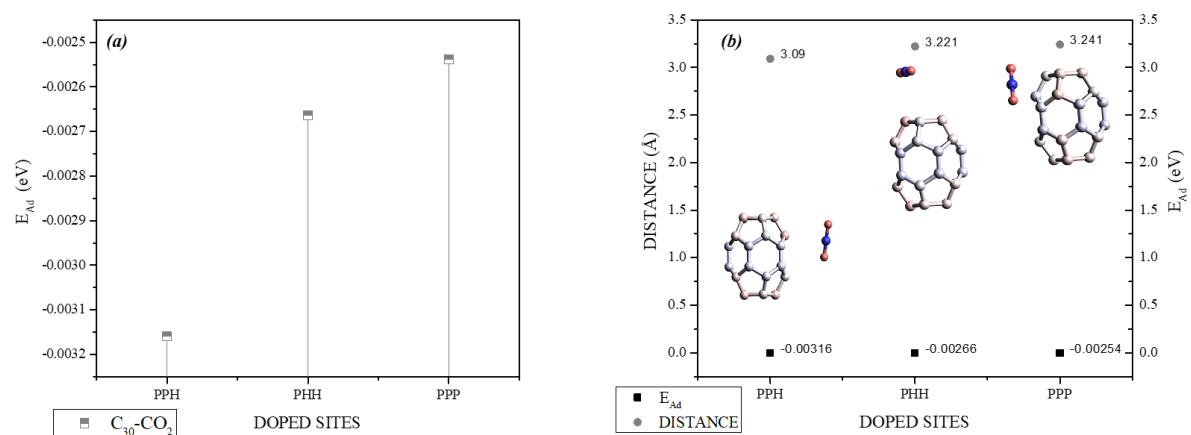


Figure 4
System $C_{30}-CO_2$: Adsorption energy (a), Ratio of adsorption energy to distance (b)
Source: Own elaboration

Table 2 presents the adsorption energy (E_{Ad}), the BSSE superposition error, the HOMO energy, the LUMO energy and the energy of the forbidden band (E_{Gap}).

Box 6

Table 2
system variables $C_{30}-CO_2$

DOPING SITES	$C_{29}X-CO_2$ (eV)	E_{Ad} TOTAL (eV)	BSSE (eV)	HOMO (eV)	LUMO (eV)	E_{gap} (eV)
PPH	$C_{30}-CO_2$	-0.003159	0.002494	-4.669	-4.236	0.433
PHH	$C_{30}-CO_2$	-0.002664	0.002234	-4.673	-4.244	0.429
PPP	$C_{30}-CO_2$	-0.0025384	0.002121	-4.686	-4.244	0.442

Source: Own elaboration

In the fullerene C_{30} , Carbon atoms have sp^2 hybridisation, which allows the formation of molecular orbitals that are distributed throughout the structure. According to band theory, the electrons in these orbitals move freely within bands formed by the overlap of these orbitals. The bonding molecular orbitals contribute to the formation of the conduction band. In materials such as metals, the valence band and conduction band can overlap, facilitating electrical conduction. In other materials, the separation between these bands is marked by a band gap, which limits electrical conductivity.

Figure 5 shows the optimised HOMO and LUMO boundary orbitals for the $C_{30}-CO_2$ system, which is related to Fukui's theory, plays a fundamental role in determining the chemical reactivity of a molecule in interaction with other molecules. The energy difference between the HOMO and LUMO, known as the HOMO-LUMO gap, corresponds to the lowest excitation energy. In the boundary orbitals, two regions with opposite signs are displayed in the wave function: a positive phase (shown in blue) and a negative phase (shown in red). These phases correspond to the electron density distribution in the molecules, where the colours indicate the alternating signs of the wave function.

Box 7

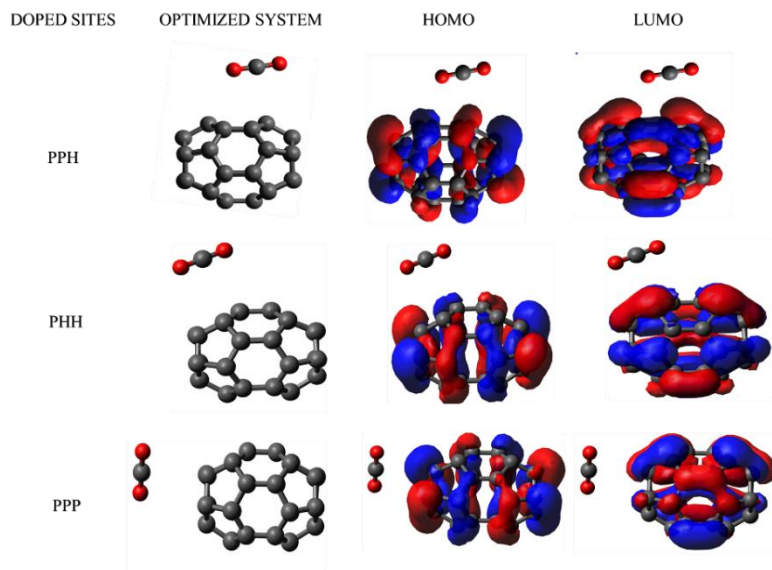


Figure 5
HOMO and LUMO boundary orbitals of the C30-CO₂ system at different doping sites

Source: Own elaboration

System C₂₉B-CO₂ and C₂₉N-CO₂

The system was calculated C₂₉B-CO₂ and C₂₉N-CO₂ after optimisation. In figure 3.3, it shows the adsorption energy of C₂₉BandCO₂, reflecting a lower to higher adsorption energy with respect to the doping sites; double pentagon ring and a hexagon ring (*PPH*), triple pentagon ring (*PPP*), double hexagon ring and a pentagonal ring (*PHH*). The relationship between distance and adsorption energy of the C₂₉B-CO₂ system. A carbon bond of theCO₂-doped fullerene structure is observed at the PPH doping site.

Box 8

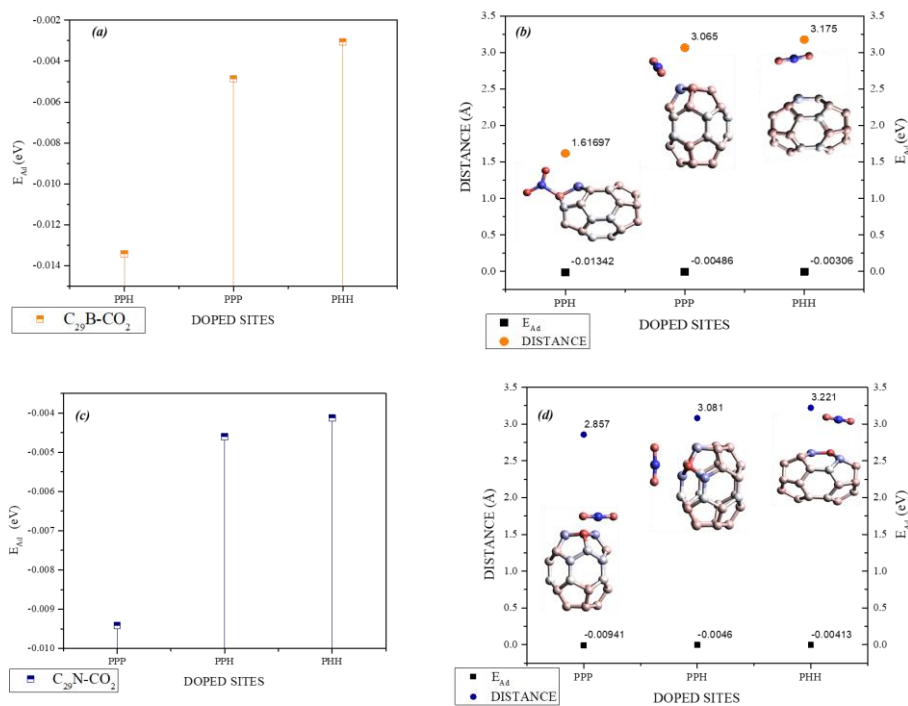


Figure 6
System C₂₉B-CO₂: Adsorption energy (a), Adsorption energy and distance ratio (b).
System C₂₉N-CO₂: Adsorption energy (c), Adsorption energy and distance ratio (d).

Source: Own elaboration

In the $C_{29}N-CO_2$ system, the interaction of $C_{29}N$ and CO_2 is shown, reflecting a lower to higher adsorption energy with respect to the doping sites; triple pentagon ring (*PPH*), triple pentagon ring (*PPP*), double hexagonal ring and a pentagonal ring (*PHH*). (see figure 6). The relationship between distance interaction and adsorption energy of the $C_{29}N$ and CO_2 system decreases, but at different doping site compared to the $C_{29}B-CO_2$ system in figure 3.3 (see figure 6). Table 3 presents the results obtained for the $C_{29}B-CO_2$ and $C_{29}N-CO_2$ systems: Adsorption Energy, HOMO, LUMO and EGap (energy gap between HOMO and LUMO). These variables have been calculated for the optimised systems at their different doping sites.

Box 9

Table 3.3
System variables $C_{29}B-CO_2$ y $C_{29}N-CO_2$

DOPING SITES	$C_{29}X-CO_2$	E_{Ad} TOTAL (eV)	BSSE (eV)	HOMO (eV)	LUMO (eV)	E_{gap} (eV)
PHH	$C_{29}B-CO_2$	-0.003060846	0.002283154	-0.584	-0.083	0.501
	$C_{29}N-CO_2$	-0.004128	0.002689	-0.594	-0.112	0.482
PPH	$C_{29}B-CO_2$	-0.013416	0.007284	-1.374	-0.887	0.487
	$C_{29}N-CO_2$	-0.004601	0.003458	-0.626	-0.081	0.545
PPP	$C_{29}B-CO_2$	-0.004862	0.003166	-0.593	-0.096	0.497
	$C_{29}N-CO_2$	-0.009413	0.003001	-0.568	-0.109	0.459

Source: Own elaboration

Figure 7 shows the optimised geometry of each of the systems, showing the distributions of the HOMO and LUMO orbitals corresponding to each doped structure.

Box 10

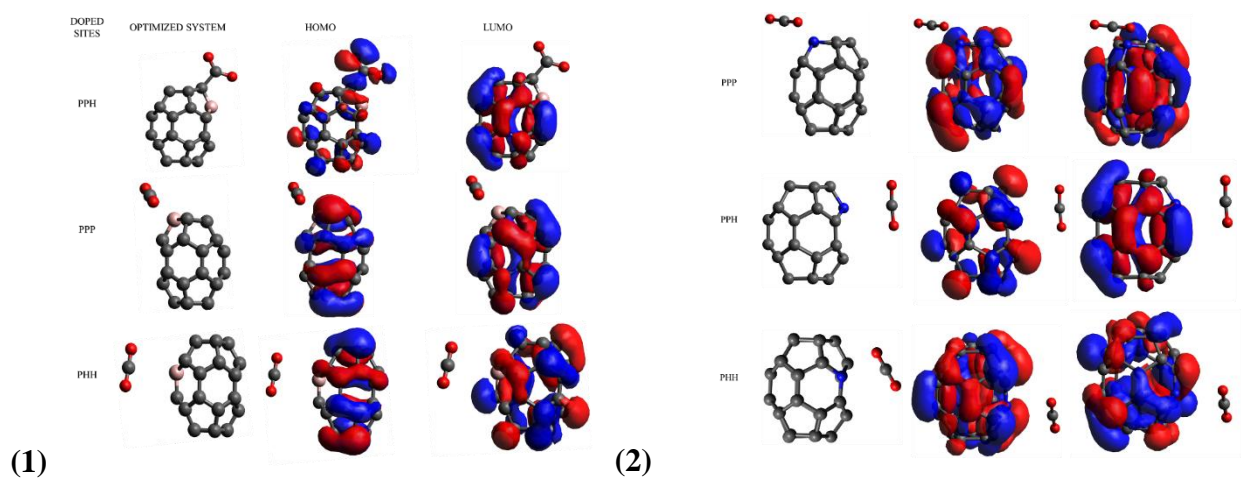


Figure 7
HOMO and LUMO boundary orbitals of the $C_{29}B-CO_2$ system at different doping sites (1)
HOMO and LUMO boundary orbitals of the $C_{29}N-CO_2$ system at different doping sites (2)

Source: Own elaboration

Conclusions

The results obtained for the adsorption energy of C_{30} and $C_{29}X$ ($X=B, N$) in the presence of CO_2 indicate that the doping site with some element has an impact on the optimisation process. However, it was observed that depending on the family group to which the element belongs, the doping site and its properties will not always be in the same order for all of them. These are due to the electronegativity, atomic size and orbital properties of the elements, which affect both the polarity and charge distribution in the system, thus modifying the CO_2 adsorption capacity in the molecular structure.

Declarations

Conflict of interest

The authors declare that they have no conflicts of interest. They have no financial interests or personal relationships that could have influenced this book.

Authors' contribution

Toxqui-De La Torre, Ana Paulina: Drafting, data analysis, figure production.

Mandujano-Ramirez, Humberto Julián: Proofreading, editing, revising results and proofreading.

Martinez-Vargas, Sergio: Spelling check, editing, proofreading, proofreading, output review and correction.

Patiño-Carachure, Cristóbal: Proofreading and editing.

Availability of data and materials

The information contained in this document is not available, prior to the data being worked on.

Funding

No funding was received.

Acknowledgements

I thank the core of the Master in Materials and Energy Engineering and my Drs. for supporting me in this research work, as well as the support received from CONAHCYT to continue contributing to the advancement of science and technology in our country.

Abbreviations

DFT	DENSITY FUNCTIONAL
GAP	THEORY BANDGAP
HOMO	HIGHEST OCCUPIED MOLECULAR
LUMO	LOWEST UNOCCUPIED MOLECULAR ORBITAL

References

Background

Adjizian, J. J., Vlandas, A., Rio, J., Charlier, J. C., & Ewels, C. P. (2016). [Ab initio infrared vibrational modes for neutral and charged small fullerenes \(C20, C24, C26, C28, C30 and C60\)](#). *Philosophical Transactions of the Royal Society A: Mathematical, Physical and Engineering Sciences*, 374(2076).

Baei, M. T., Koohi, M., & Shariati, M. (2018). [Structure, stability, and electronic properties of AlP nanocages evolved from the world's smallest caged fullerene C20: A computational study at DFT](#). *Journal of Molecular Structure*, 1159, 118–134.

Bhakta, P., & Barthunia, B. (2020). [Fullerene and its applications: A review](#). *Journal of Indian Academy of Oral Medicine and Radiology*, 32(2), 159.

Fekri, M. H., Bazvand, R., Solymani, M., & Mehr, M. R. (2020). [Adsorption Behavior, Electronical and Thermodynamic Properties of Ornidazole Drug on C60 Fullerene Doped with Si, B and Al: A Quantum Mechanical Simulation](#). *Physical Chemistry Research*, 9(1), 151–164.

Grądzka, E., Wysocka-Żołopa, M., & Winkler, K. (2020). [Fullerene-Based Conducting Polymers: n - Dopable Materials for Charge Storage Application](#). *Advanced Energy Materials*, 10(40).

- Hasanah, D., . W., Mulyani, S., & Widhiyanti, T. (2024). [Multiple Representations Analysis of Chemical Bonding Concepts in General Chemistry Books](#). KnE Social Sciences.
- Paul, D., Mane, P., Sarkar, U., & Chakraborty, B. (2023). [Yttrium decorated fullerene C30 as potential hydrogen storage material: Perspectives from DFT simulations](#).
- Shetti, N. P., Mishra, A., Basu, S., & Aminabhavi, T. M. (2021). [Versatile fullerenes as sensor materials](#). In *Materials Today Chemistry* (Vol. 20). Elsevier Ltd.
- Tománek, D. (2014). [Guide Through the Nanocarbon Jungle](#). Morgan & Claypool Publishers.
- Yang, Y., Sun, A., & Gu, W. (2021). [Sensing behavior of pristine and doped C70 fullerenes to mercaptopurine drug: a DFT/TDDFT investigation](#). *Structural Chemistry*, 32(1), 457–468.

Basics

- Apebende, C. G., Ogunwale, G. J., Louis, H., Benjamin, I., Kadiri, M. T., Owen, A. E., & Manicum, A.-L. E. (2023). [Density functional theory \(DFT\) computation of pristine and metal-doped MC59 \(M = Au, Hf, Hg, Ir\) fullerenes as nitrosourea drug delivery systems](#). *Materials Science in Semiconductor Processing*, 158, 107362.
- Babu, D. J., Bruns, M., Schneider, R., Gerthsen, D., & Schneider, J. J. (2017). [Understanding the influence of N-doping on the CO₂ adsorption characteristics in carbon nanomaterials](#). *Journal of Physical Chemistry C*, 121(1), 616–626.
- Bai, H., Ji, W., Liu, X., Wang, L., Yuan, N., & Ji, Y. (2013). [Doping the buckminsterfullerene by substitution: Density functional theory studies of C59X \(X = B, N, Al, Si, P, Ga, Ge, and As\)](#). *Journal of Chemistry*.
- Canales, M., Ramírez-de-Arellano, J. M., & Magana, L. F. (2016). [Interaction of a Ti-doped semi-fullerene \(TiC30\) with molecules of CO and CO₂](#). *Journal of Molecular Modeling*, 22(9).
- Giustino, F. (2014). *Materials modelling using density functional theory: properties and predictions*. Oxford University Press.
- Harismah, K., Hassan, A., Nassar, M. F., Hamid, O. T., & Zandi, H. (2023). [Carbon Dioxide Uptake by a Polonium-Doped Fullerene: Computational Analyses](#). *Biointerface Research in Applied Chemistry*, 13(5).
- Khan, A. A., Ahmad, R., Ahmad, I., & Su, X. (2021). [Selective adsorption of CO₂ from gas mixture by P-decorated C24N24 fullerene assisted by an electric field: A DFT approach](#). *Journal of Molecular Graphics and Modelling*, 103.

Support

- Boys, S. F., & Bernardi, F. (1970). [The calculation of small molecular interactions by the differences of separate total energies](#). Some procedures with reduced errors. *Molecular Physics*, 19(4), 553–566.
- Burke, K. (2007). [The ABC of DFT](#).
- Neese, F. (2018). [Software update: the ORCA program system, version 4.0](#). *WIREs Computational Molecular Science*, 8(1).
- Khan, A. A., Ahmad, R., Ahmad, I., & Su, X. (2021). [Selective adsorption of CO₂ from gas mixture by P-decorated C24N24 fullerene assisted by an electric field: A DFT approach](#). *Journal of Molecular Graphics and Modelling*, 103.
- Seeman, J. I. (2022). [Kenichi Fukui, Frontier Molecular Orbital Theory, and the Woodward-Hoffmann Rules. Part III](#). *Fukui's Science and Technology, 1918–1965†**. *The Chemical Record*, 22(4).